JOURNAL OF SOLID STATE CHEMISTRY 93, 134–145 (1991)

Spectrochemical Investigations of Ultrafine Amorphous and Crystalline Rare Earth Iron Garnets

V. K. SANKARANARAYANAN AND N. S. GAJBHIYE*

Department of Chemistry, Indian Institute of Technology, Kanpur-208 016, India

Received July 23, 1990; in revised form February 28, 1991

The absorption bands caused by the lattice vibrations and electronic transitions due to tetrahedral and octahedral Fe^{3+} in ultrafine submicron-sized rare earth iron garnets (RIG) prepared by the thermal decomposition of citrate precursors are studied to elucidate the local molecular structure. The ultrafine garnet samples consisting of 1.0- to 1.5-nm sized crystallites are X-ray amorphous and show evidence for greater specific volume compared to crystalline garnets in XRD and IR studies. An energy level scheme of $3d^5$ for Fe^{3+} in tetrahedral and octahedral coordination in these ultrafine crystallites is proposed. The ligand-field parameters suggest a decrease of octahedral Fe–O distance and an increase of tetrahedral Fe–O distance. The Mössbauer isomer shift values show interesting correlations with Racah parameters and confirm the variation of Fe–O distances in the amorphous state. The ultrafine crystalline materials comprising 10- to 35-nm sized crystallites exhibit absorption frequencies and ligand-field parameters comparable to crystalline garnets.

1. Introduction

The cation distributions in various garnets have been the subject of various studies in the past using different techniques (*1–4*). The crystalline garnet, $R_3Fe_5O_{12}$ consists of alternating distorted polyhedra, FeO_4 tetrahedra (*d*-site) and FeO_6 octahedra (*a*-site), which share corners to form a continuous three-dimensional framework (*5–8*). The oxygen atoms in the framework also define distorted triangular dodecahedra consisting of eight oxygens, RO_8 (*c*-site), which coordinate rare earth, R^{3+}, cations (Fig. 1) Many rare earth ions have electronic absorptions due to the weak spin forbidden $f \rightarrow f$ transitions and are observed in the near IR to UV region in garnet (*9, 10*). The optical absorption at short wavelengths (10,000 to 50,000 cm^{-1}) in rare earth iron garnets is dominated by two types of electronic transitions due to Fe^{3+} ions (*11, 12*). First there are discrete lines due to crystal-field transitions of Fe^{3+} ions in tetrahedral and octahedral sites in the garnet lattice. Second, there is much stronger absorption due to a charge-transfer process involving the shift of an electron from the oxygen ligands to the central Fe^{3+} ions which appears above 35,000 cm^{-1} (*13*). The longer wavelength, $\nu < 1000$ cm^{-1}, region is dominated by vibrational lattice modes. A factor group analysis has been carried out to predict the lattice modes (*14*).

* To whom correspondence should be addressed at present address: University Department of Chemistry, University of Bombay, Vidyanagari, Santacruz (East) Bombay 400 098.

0022-4596/91 $3.00

This analysis predicts 17 IR active modes of which the powder IR spectra of crystalline garnets show 10 frequencies. The highest frequency fundamental vibration is due to the triply degenerate ν_3 asymmetrical vibration of the tetrahedral FeO_4 group. The degree of removal of the degeneracy of ν_3 is a measure of the distortion of the tetrahedron (*15*). The Mössbauer spectra yield valuable information on the chemical bonding of iron at the structural sites, like ligand-field and IR spectra (*16, 17*) do. The isomer shift is a function of the oxygen coordination numbers at Fe^{3+} sites and the cation–anion distances. An interesting question is the relationship between the isomer shift of ^{57}Fe and the Racah parameter, B, of Fe; that is, a decrease of isomer shift has been shown to be in agreement with a decrease of B value (*3*).

All the above-mentioned studies pertain to single-crystal or bulk polycrystalline garnets. The ultrafine submicron-sized rare earth iron garnets, however, have not been investigated by spectrochemical methods with a view to elucidate the local molecular structure. As a matter of fact, fine particles offer as attractive an avenue for the study of magnetic properties of surfaces as do thin films (*18*). Ultrafine particles in the smallest size range may be effectively all surface (*19*). Therefore, in the present study, a consistent interpretation of the IR and optical spectra of ultrafine, amorphous, and crystalline, rare earth iron garnets $R_3Fe_5O_{12}$ where R = Sm, Tb, Dy, Ho, Er, Yb, (YNd) and (YGd), is attempted to elucidate the local molecular structure in low dimensions. Based on the measurements of the absorption spectra, the ligand-field parameters Δ(oct) and Δ(tet) and the Racah parameters B(oct) and B(tet) are calculated and an attempt is made to correlate these parameters with the cation–anion distances in oxygen polyhedra. It may be mentioned that, while the relationship of Δ with the cation–anion distances is reasonably well established, B and C may not be as good indicators of the cation–anion distances. The study also illustrates the relationship between the Racah parameters and the isomer shifts obtained from Mössbauer spectra.

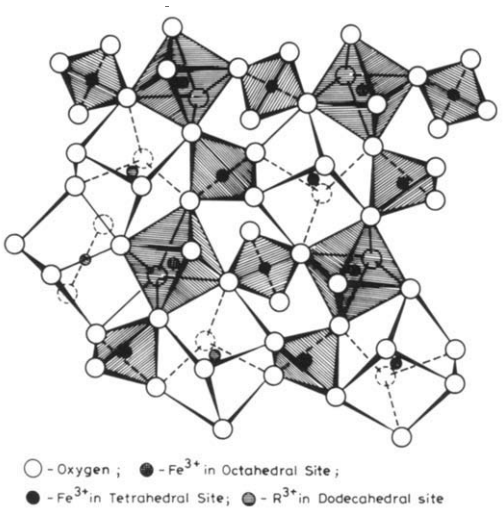

FIG. 1. Arrangement of oxygen polyhedra in the garnet structure.

2. Experimental Aspects

The ultrafine submicron-sized, rare earth iron garnets were prepared by thermal decomposition of citrate precursor $R_3Fe_5(cit)_{25} \cdot (36 + n)H_2O$. The method of preparation, chemical analysis, and thermal decomposition studies of citrate precursors are described elsewhere (*20, 21*). On decomposition in air atmosphere, the precursors yield X-ray amorphous ultrafine particles at 450°C which crystallize above 600°C. The amorphous RIG materials were heat-treated in air atmosphere at various temperatures between 450 and 1000°C for 4 hr each.

XRD patterns were obtained with a Rich Seifert Isodebyflex Model 2002 Diffractometer using Nickel-filtered Cu$K\alpha$ radiation. The IR spectra of the various heat-treated samples were recorded on a Perkin–Elmer

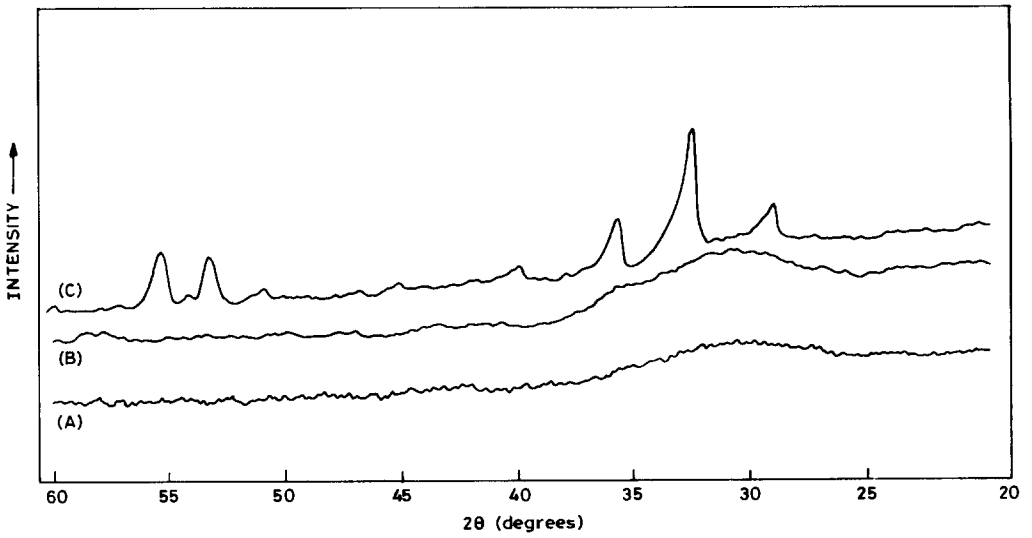

FIG. 2. XRD patterns of ultrafine garnet materials heat-treated at (A) 450°C (B) 600°C and (C) 700°C.

783 spectrophotometer using the KBr pellet technique in the frequency range of 4000 to 200 cm^{-1}. The measurements in the UV–visible region were performed in the range 8000 to 30,000 cm^{-1} using a Shimadzu UV-160 spectrophotometer by the reflectance technique. The Mössbauer spectra were studied at constant acceleration in conjunction with a Nuclear Data Instruments ND60 multichannel analyzer using a ^{57}Co source in a Rhodium matrix. The experimentally observed Mössbauer spectra were curve fitted by a least-squares method using a computer program and assuming Lorentzian lineshapes.

3. Results and Discussion

3.1 Nature of Ultrafine Amorphous and Crystalline RIG

The ultrafine particles of rare earth iron garnets were characterized in detail by XRD, TEM, and BET surface area measurements and presented elsewhere (*21*). In the heat-treatment temperature range 450 to 600°C, the RIG materials exhibit a broad hump corresponding to d_{420} in the range d = 0.20 to 0.35 nm which indicates the absence of crystalline periodicity and the existence of a strained amorphous state and represented for HoIG in Fig. 2. Application of the classical Scherrer formula for XRD line broadening yields a crystallite size of 1.0 to 1.5 nm. The crystallites exist as nonporous aggregates bound together by primary bonds as shown by the BET and TEM studies (*21*). Above 600°C the crystallites grow to 10- to 35-nm monoliths with negligible lattice strain. The greater d-spacing value for 1.0- to 1.5-nm sized crystallites (amorphous state) compared to 10 to 35 nm (crystalline state) correspond to the relative increase of specific volume of the RIG lattice. The larger size induced strain that is suggested to be responsible for the garnet lattice becoming distorted and unstable. Such lattice expansion with decreasing particle size has been reported in various metallic and nonmetallic fine particle systems (*22, 23*). The distortion may be attributed to crystal symmetry and

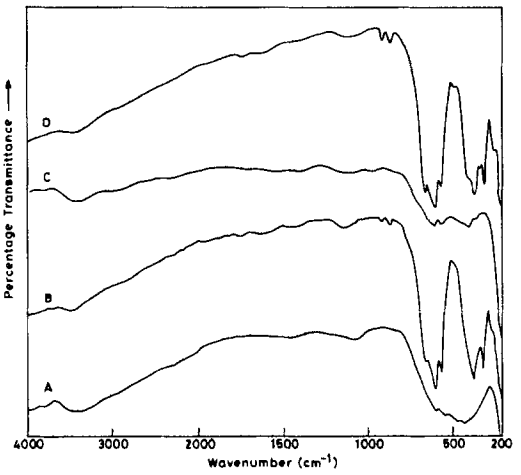

FIG. 3. IR spectra of ultrafine garnet materials heat-treated at various temperatures (A) 450°C (B) 900°C for DyIG and (C) 450°C (D) 900°C for HoIG.

surface effects or multitwinning in the structure of ultrafine crystallites.

3.2 Infrared Spectral Studies

The IR spectra of ultrafine RIG materials in amorphous and crystalline states are represented by DyIG and HoIG in Fig. 3 and the absorptions are given in Table I. The materials show two bands in the 700- and 300-cm^{-1} region due to lattice modes. The band at higher frequency consists of three peaks corresponding to a ν_3 fundamental vibration of the FeO_4 tetrahedron in ultrafine crystalline DyIG and HoIG materials. Due to the distorted nature of the FeO_4 tetrahedron in garnet structure, the splitting of bands is expected and observed in ultrafine crystalline materials. The ultrafine amorphous materials comprising crystallites of 1.0- to 1.5-nm size, prepared at 450 to 600°C show broad absorption in this region apparently due to the dangling bonds in the amorphous structure. The broad bands exhibited by the amorphous materials instead of six sharp lines observed in crystalline materials could also be an indication of relatively less distortion of the tetrahedra in the amorphous state. Interestingly, broad bands are observed at 435 cm^{-1} and 410 cm^{-1} in amorphous DyIG and HoIG materials which are shifted from the original positions of the crystalline materials. A careful analysis of IR absorptions of various rare earth iron garnet materials indicate the presence of 435-cm^{-1} absorption in lighter garnets such as SmIG, EuIG, and GdIG (*14*). Therefore it appears that the FeO_4 tetrahedra in the amorphous state have comparable symme-

TABLE I

IR LATTICE ABSORPTIONS OF ULTRAFINE DyIG AND HoIG MATERIALS HEAT-TREATED AT VARIOUS TEMPERATURES

Ultrafine DyIG materials lattice absorption (cm^{-1})			Polycrystalline DyIG (*14*) (cm^{-1})	Ultrafine HoIG materials lattice absorption (cm^{-1})			Polycrystalline HoIG (*14*) (cm^{-1})
450	600	700		450	600	700	
610	610	670	647	610	630	670	655
		610				615	600
555	555	570	597	570	565	570	565
			562				
435	435			410	410		
		375	380			380	386
		350	365			370	330
		320	330			340	308
			309			315	

try to that of the crystalline state of lighter rare earth iron garnets. Besides, it is known that the lighter RIG materials in the crystalline state possess an expanded lattice compared to that of heavier rare earth iron garnets. Hence, the appearance of 435-cm^{-1} absorption confirms the larger specific volume in the amorphous RIG materials. Moreover, lattice absorption bands show a relative shift to lower frequencies in the amorphous state, which again indicate an increase of specific volume because the lighter rare earth iron garnets (which have larger specific volume) show low frequency shift of the lattice absorptions.

The absorption bands between 800 and 2400 cm^{-1} are believed to be due to multiphonon processes in which one photon generates two or more phonons. The two-phonon and three-phonon processes produce absorption peaks in RIG materials which are nearly equal to $2\,\bar{\nu}_3$ and $3\,\bar{\nu}_3$ peaks of the FeO_4 group. This is an intrinsic feature of the RIG materials (*24*) and is not caused by trace impurities as reported in the literature (*15*).

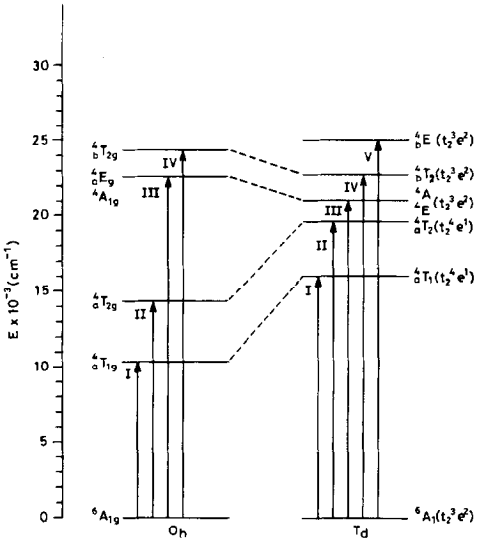

FIG. 4. Energy-level diagram of octahedral and tetrahedral Fe^{3+} in ultrafine crystalline ErIG consisting of 10- to 35-nm crystallites.

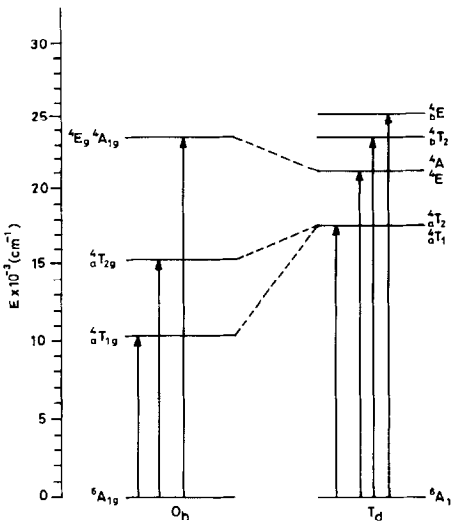

FIG. 5. Energy-level diagram of octahedral and tetrahedral Fe^{3+} in ultrafine amorphous ErIG consisting of 1.0- to 1.5-nm crystallites.

3.3 Reflectance Spectral Studies of Ultrafine, Amorphous, and Crystalline RIG Materials

The optical reflectance spectra of ultrafine amorphous and crystalline RIG materials show several weak absorption bands. The energy level schemes of $3d^5$ for the Fe^{3+} ion in tetrahedral and octahedral coordination in these ultrafine crystalline and amorphous materials are proposed and shown in Figs. 4 and 5. The observed positions of these bands are presented in Table II and are shown in Fig. 6. The observed absorptions of the Fe^{3+} ion in octahedral and tetrahedral sites of the garnet structure are due to the electronic transitions from the ground state $^6A_1$ to the excited states $^4_aT_1$, $^4_aT_2$, $^4A_1{}^4_aE_g$, $^4_bT_2$, ^4_bE and $^4_bT_1$. These transitions (*3, 9*) are forbidden and hence of relatively low intensity. It should be mentioned that the lack of inversion at the tetrahedral site relaxes the parity rule and results in higher intensities

TABLE II

OBSERVED ENERGIES OF THE ABSORPTION MAXIMA OF Fe^{3+} IN GARNETS AT 298 K

$R_3Fe_5O_{12}$	Heat treatment temperature (°C)	Absorption maxima (cm^{-1})						
$Y_3Fe_5O_{12}$	Pure YIG (*3*)	10,500	14,300	16,400	19,500	20,800/ 21,400	22,800	25,700
$Sm_3Fe_5O_{12}$	450	10,565	16,105	17,986		21,668	23,697	25,575
	600	10,304	15,105	17,966		21,332	23,753	25,445
	900	11,099	14,719	16,511	19,672	21,102	22,765	25,255
$Tb_3Fe_5O_{12}$	450	10,846	15,200	17,921		21,413	23,419	25,510
	600	—	—	17,825		21,459	23,585	25,575
	900	10,846	14,634	16,511	19,618	21,042	22,848	25,225
$Dy_3Fe_5O_{12}$	450	11,110	15,540	17,657		21,882	23,535	25,316
	600	11,110	—	17,668		21,809	23,419	25,253
	900	11,050	14,316	16,260	19,579	21,124	22,926	25,310
$Ho_3Fe_5O_{12}$	450	—	15,375	17,637		21,274	23,755	25,510
	600	—	15,432	17,637		21,505	23,529	25,510
	900	11,111	14,420	16,340	19,450	21,048	22,738	25,271
$Er_3Fe_5O_{12}$	450	10,268	15,251	17,544		21,552	23,697	25,510
	600	10,246	15,244	17,762		21,612	23,585	25,575
	900	10,920	14,035	16,247	19,675	21,115	22,918	25,375
$Yb_3Fe_5O_{12}$	450	10,235	15,250	17,668		21,219	23,641	25,510
	600	10,235	15,385	17,668		21,322	23,691	25,575
	900	10,799	14,035	16,103	19,536	21,032	22,815	25,225
$Y_2NdFe_5O_{12}$	450	10,758	15,337	17,606		21,645	23,585	25,445
	600	—	15,244	17,528		21,299	23,585	25,445
	900	10,758	14,641	16,452	19,555	21,158	22,912	25,225
$Y_2GdFe_5O_{12}$	450	10,588	15,385	17,721		21,322	23,529	25,510
	600	—	15,290	17,544		21,505	23,529	25,210
	900	11,030	14,352	16,327	19,525	21,132	23,726	25,315

of tetrahedral bands. In ultrafine amorphous RIG materials the tetrahedral absorptions are relatively more intense compared to the octahedral ones and many of the octahedral absorptions are missing. Nevertheless, the assignments of tetrahedral bands are more complicated because no good samples bearing only the tetrahedral Fe^{3+} ion, whose synthesis is considered difficult, are available (*3*). The ligand-field energies are calculated using the energy equations of Fe^{3+} ions. The fit was done using Tanabe–Sugano matrices with the parameters (*25*)

B_0 (free ion) = 950 cm^{-1};

C/B = 5.0; Δ/B(oct) ~ 20.0 and Δ/B(tet) ~ 12.0.

The B(tet) and B(oct) values (Racah parameters) are calculated from Δ-independent transitions and the Δ(oct) and Δ(tet) (ligand-field parameters) values from $^4_aT_1$ and $^4_aT_2$ bands. The parameters Δ and B are both calculated using the energy equations which utilize the C/B ratio. Therefore the calculated parameters are sensitive to this ratio. Hence the C/B ratio of 5.0 was chosen in such a way that the frequency assignments of all the RIG materials could be done with minimum ambiguity.

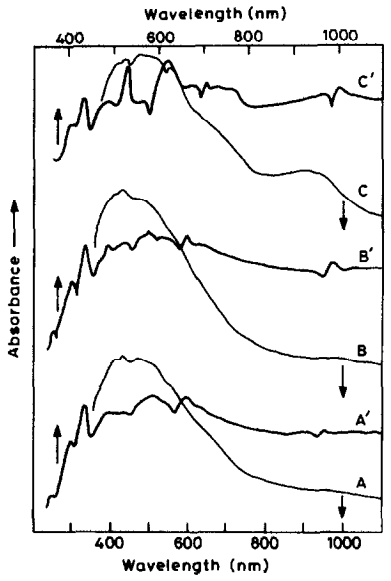

FIG. 6. Reflectance spectra of ultrafine ErIG materials heat-treated at (A) 450°C (B) 600°C (C) 900°C; A', B' and C' are the respective derivative spectra.

3.3.1 Assignment of the energy levels of octahedral Fe^{3+}. In the reflectance spectra of ultrafine amorphous and crystalline RIG materials (Fig. 6) the absorption at ~23,630 cm^{-1} is relatively intense and has been assigned to a transition to the Δ-independent levels $^4A_{1g}, {}^4_aE_g$. From the energy E of the $^4A_{1g}, {}^4_aE_g$ levels the interelectronic repulsion parameter of octahedral Fe^{3+}, B(oct), can be calculated using the equation of Tanabe and Sugano (*25*),

$$E(^4A_{1g}, {}^4_aE_g) = 10B + 5C = 35B.$$

Using the average E = 23,632 cm^{-1}, and C/B = 5, B(oct) is found to be 675.2 cm^{-1} for the amorphous RIG materials prepared at 450°C, whereas for crystalline RIG it is reported and observed to be B(oct) = 650 ± 10 cm^{-1} (Table III). Single-crystal absorption spectra of natural garnets spessartine, $Mn_3(AlFe^{3+})_2Si_3O_{12}$, grossular, $Ca_3(AlFe^{3+})_2Si_3O_{12}$, pyrope, $Mg_3(AlFe^{3+})_2Si_3O_{12}$, and andradite, $Ca_3Fe^{3+}_3Si_3O_{12}$, confirm this assignment (*26, 27*) as they reveal the Δ-independent transition to $^4A_{1g}, {}^4_aE_g$ to be at 22,700–23,300 cm^{-1}.

The absorptions around 10,600 and 15,300 cm^{-1} in the optical spectrum of amorphous RIG material are assigned to the transitions $^6A_{1g} \rightarrow {}^4_aT_{1g}$ and $\rightarrow {}^4_aT_{2g}$ of the octahedral Fe^{3+}. The assignment of these two lowest energy bands is in accordance with the literature and measured at 11,300 cm^{-1} and 15,000 cm^{-1} in the YCa garnets and 11,600 and 15,000 cm^{-1} in andradite (*4*). The ligand field parameter Δ(oct) = 15,900 cm^{-1} is calculated for these transitions assuming B(oct) = 675 cm^{-1} (Table III). According to Tanabe–Sugano diagrams, the energies of these two lowest energy levels decrease with increasing ligand-field parameter Δ(oct), i.e., with decreasing octahedral cation–anion distance. The crystal structural refinements show that the cation–anion distances are 1.937 Å in YAG, 1.995 Å in YGG, 2.019 Å in YIG, and 2.024 Å in andradite (*7, 8*). According to these results and assuming that the ligand-field parameter, Δ(oct) increases with decreasing cation–anion distance, the ${}^4_aT_{1g}$ and ${}^4_aT_{2g}$ levels would have the least energy in ultrafine amorphous RIG materials. But the observed energies are greater than or equal to the energies of other garnet systems. This may be the result of large B values obtained for the present system. Moreover, other spectroscopic evidences of ultrafine amorphous materials also indicate a decrease of octahedral bond distance which would mean an increase of Δ value. The observation of these low energy absorption bands of the octahedral Fe^{3+} indicates the sensitivity of reflectance spectra, whose Mössbauer spectra (*21*) reveal only the characteristic doublet of tetrahedral Fe^{3+}. This shows that the optical absorption spectra are very sensitive for small amounts of Fe^{3+} in a certain position of the garnet structure.

3.3.2 Assignment of energy levels of tetrahedral Fe^{3+}. The band at ~21,400 cm^{-1}

TABLE III

RACCAH PARAMETER B (cm^{-1}) AND LIGAND FIELD PARAMETERS Δ (cm^{-1}) AND MOSSBAUER ISOMER SHIFT δ (mm/s) FOR ULTRAFINE RIG MATERIALS

$R_3Fe_5O_{12}$	Heat treatment Temperature (°C)	B(tet) values $^4A_1, {}^4_aE$	$^4_bE_g$	Δ (tet) $^4_aT_1, {}^4T_2$	B(oct) $^4A_{1g}, {}^4E_g$	Δ (oct) $^4T_1$	$^4T_2$	Isomer shift δ (mm/s) (w.r.t. natural fe) Tet	Oct
$Sm_3Fe_5O_{12}$	450	619	609	—	677	15,839	16,092	0.31	
	600	609	606	4995	679	16,187	16,186	0.33	
	900	603	602	7107	650	14,321	15,328	—	—
$Tb_3Fe_5O_{12}$	450	612	607	5064	669	15,471	16,100	—	
	600	613	609	5168	674	—	—	—	
	900	601	601	7178	653	14,582	15,422	0.16	0.38
$Dy_3Fe_5O_{12}$	450	610	603	5269	672	15,548	15,822	0.33	
	600	591	—	5370	669	15,480	16,100	0.33	
	900	604	603	7358	656	14,371	15,775	0.19	0.44
$Ho_3Fe_5O_{12}$	450	608	607	5370	672	—	15,888	0.34	
	600	614	607	5370	679	—	15,548	0.34	
	900	601	602	7390	650	14,309	15,660	0.20	0.39
$Er_3Fe_5O_{12}$	450	616	607	5470	677	16,145	15,882	0.40	
	600	620	609	5235	674	16,049	15,788	0.33	
	900	603	604	7140	655	14,505	16,088	0.20	0.35
$Yb_3Fe_5O_{12}$	450	606	620	—	675	16,100	15,680	0.30	
	600	609	607	5337	677	16,179	15,778	0.29	
	900	601	600	7284	652	14,630	16,088	0.21	0.46
$Y_2NdFe_5O_{12}$	450	618	606	5403	674	15,324	15,685	0.33	
	600	608	606	5487	674	—	15,811	0.34	
	900	605	601	7259	655	14,672	15,414	0.20	0.44
$Y_2GdFe_5O_{12}$	450	609	607	5269	672	16,030	15,535	0.33	
	600	614	607	5470	672	—	15,640	0.30	
	900	604	603	7290	649	14,392	15,735	0.15	0.35

in various ultrafine amorphous RIG materials is interpreted as the first Δ-independent level $^4A_1, {}^4_aE$ of octahedral Fe^{3+} (Table II). This band splits into two maxima at 20,700 and 21,300 cm^{-1} in crystalline RIG materials. The splitting can be due to two effects: (i) The influence of covalency may lift the degeneracy of the two levels $^4A_1$ and ^4_gE(ii) The considerable distortion of the FeO_4 tetrahedron may cause an additional splitting of the tetrahedral levels. An argument in the same line leads to the interesting conclusion that these tetrahedra are relatively less distorted in the amorphous state or in the ultrafine amorphous RIG materials. In crystalline garnets the distortion of the tetrahedron is greater than that of the octahedron. Assuming an average energy of 21,400 cm^{-1} and using the energy equation $E = 10B + 5C$, B(tet) is calculated to be 610 cm^{-1} for RIG materials prepared at 450°C, which is lower than the B(oct) value (Table III) and is comparable to B(tet) = 600 cm^{-1} for crystalline garnets reported in the literature (*3*). The absorption band observed at ~25,600 cm^{-1} can be assigned to the second Δ-independent level ^4_bE of the tetrahedral Fe^{3+} which is reported for YIG at 25,200 cm^{-1}. Using B(tet) = 610 cm^{-1}, the calculated energy value is 25,800 cm^{-1}. The B(tet) value is calculated using this transition and is presented in Table III.

The intense band at ~23,600 cm^{-1} in all the ultrafine amorphous RIG materials can

TABLE IV

AVERAGE VALUES OF REFLECTANCE SPECTRA PARAMETERS

Heat treatment temperature (°C)	⟨B(tet)⟩	⟨B(oct)⟩	⟨Δ(tet)⟩	⟨Δ(oct)⟩	Δ(tet)/Δ(oct)
450	610.3	675.2	5315	15,888	0.34
600	609.9	674.2	5288	15,940	0.33
900	602.8	652.5	7231	15,080	0.48

be assigned, though uncertainly, to the ${}^4_aT_2$ level of tetrahedral Fe^{3+}. The calculation using B(tet) = 610 cm^{-1} yields an energy ~23,200 cm^{-1} for the ${}^4_aT_2$ level. The corresponding absorption band would be hidden by the intense transition ${}^6A_{1g} \rightarrow {}^4A_{1g}, {}^4E_g$ of octahedral Fe^{3+}. However, the calculated B(tet) values using this absorption are in the range 615–620 cm^{-1} and are comparable to the B(tet) values obtained from other absorptions justifying the assignment of the band (Table III).

The low energy transitions ${}^6A_1 \rightarrow {}^4_aT_1$ and ${}^6A_1 \rightarrow {}^4_aT_2$ are expected in the crystalline RIG materials at about 16,200 cm^{-1} and 19,600 cm^{-1}, respectively. However, in ultrafine amorphous RIG materials, a single absorption is observed at 17,600 cm^{-1} that is much higher than the crystalline garnet value of 16,200 cm^{-1}. Assuming B(tet) = 610 cm^{-1}, the ligand field parameter Δ(tet) ~5300 cm^{-1} is obtained for amorphous RIG materials and is given in Table III. The Δ-values obtained for amorphous RIG are rather low compared to the crystalline RIG value of Δ ~ 7200 cm^{-1}. The decrease in Δ-value is an indication of an increase of cation–anion (Fe^{3+}–O) distance in the tetrahedron which means relatively less distortion in the amorphous state compared to the existing distortion in crystalline garnets and is also ascertained by the absence of splitting of energy levels.

3.3.3 Interpretation of the ligand field parameters. The average values of the ligand field parameters are shown in Table IV. There is a shift of absorption frequencies in ultrafine RIG materials in the amorphous state compared to the crystalline state. The substitution of lighter rare earth ions (larger R^{3+} ions) in the garnet lattice leads to the expansion of dodecahedra and thereby expansion of the lattice (*9*). The shift to higher energy values in lighter rare earth iron garnets results from the increase in specific volume or expansion of the lattice. Therefore in the amorphous state, the blue shift of energy values and the overall increase of specific volume compared to crystalline garnet lattice suggests the rearrangement R^{3+}–O, Fe^{3+}_a–O, and Fe^{3+}_d–O bond distances and the included bond angles. As shown by the structure refinements (*7, 8*) the bond angle opposite to the shared edge of the tetrahedron (ideally 109°25′) varies between 98 and 96° in YIG and 102.64° in andradite $Ca_3Fe_2Si_3O_{12}$, whereas the octahedral bond angle (ideally 90.00°) opposite to the shared edges varies between 83.62° in YIG and 91.12° in andradite. The considerable reduction of Δ(tet) values in the amorphous state compared to crystalline values shows an increase of Fe–O bond distance and the absence of peak-splitting indicates relatively distortion free FeO_4 tetrahedra, whereas the increase of the ligand-field parameter of octahedral Fe^{3+}, Δ(oct), suggests a decrease of the Fe–O bond distance. The Δ(tet)/Δ(oct) value in amorphous RIG materials is ~0.34, which differs substantially from the ideal value of 0.44 (*3*). Actually, the Fe^{3+}–O bond

distances in octahedral sites are appreciably reduced and those in the tetrahedral site increase, implying a larger field for the octahedral sites formed and thus reducing the value of the ratio.

3.4 Racah Parameter B, Isomer Shift δ and Garnet Structure

According to Jorgensen (*28*), the Racah parameter B decreases with increasing radial expansion of the d-electron functions of the cations, caused, at least in part, by cation–anion orbital overlap. In the crystalline garnet structure, this overlap is expected to be stronger in the tetrahedron because of the smaller tetrahedral cation–anion distances. In YIG and andradite, tetrahedral Fe^{3+}–O distances are 1.866 Å, whereas the octahedral Fe^{3+}–O distances are 2.019 and 2.024 Å, respectively (*7, 8*). According to this model, B(tet) should be smaller than B(oct). One of the most important Mössbauer parameters for the discussion of chemical bonding is the isomer shift, δ, which is about twice as large for octahedral (δ = 0.47 mm/sec) as for the tetrahedral (δ = 0.24 mm/sec) Fe^{3+} in RIG. These differences are well understood in terms of different cation–anion distances resulting in an increased s-electron density at the tetrahedral position.

Correlating ligand-field and Mössbauer parameters one can conclude the following. The isomer shift δ depends mainly on the variations of s-electron density at the nucleus whereas B reflects changes in d-electron functions. In the MO-bonding model, the s-electrons, especially $4s$, form σ-bonds with the ligand σ-orbitals which are strongly influenced by cation–anion distances. Thus, the isomer shift, δ, is very sensitive to variations in σ-bonding. Nevertheless, a radial expansion of $3d$ orbitals causes a diminished shielding effect of the d electrons and thus an increase of s-electron density at the nucleus. Thus, a decrease of B is in agreement

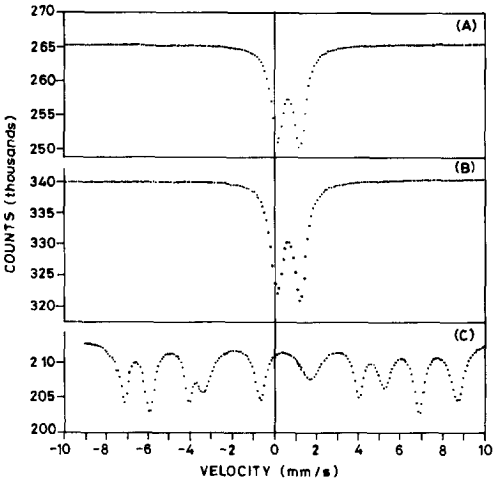

FIG. 7. Mössbauer spectra of ultrafine HoIG materials heat-treated at (A) 450°C (B) 600°C and (C) 900°C.

with a decrease of the isomer shift in crystalline RIG. The smaller B(tet) and δ(tet) values with respect to B(oct) and δ(oct) values are also in good agreement with these considerations.

In crystalline garnets the Racah parameters reported (*3*) are B(tet) = 600 cm^{-1} and B(oct) = 650 cm^{-1}. In ultrafine amorphous RIG materials, the Raccah parameters are B(tet) = 615 cm^{-1} and B(oct) = 675 cm^{-1} (Table IV). The B-value decreases with increasing radial expansion of d-electron functions of the cation Fe^{3+}, caused by the Fe^{3+}–O^{2-} (cation–anion) overlap. Therefore, the expected cation–anion overlap is larger in FeO_4 tetrahedra than in FeO_6 octahedra.

The isomer shift of Fe^{3+} in both positions shows distinct differences in crystalline and amorphous garnets as represented in the Mössbauer spectra for $Ho_3Fe_5O_{12}$ in Fig. 7. In the amorphous state, only a single doublet is observed with isomer shift (δ = 0.34 mm/sec) less than the octahedral value (δ = 0.47 mm/sec) and greater than the tetrahedral value (δ = 0.24 mm/sec) of crystalline garnets (with respect to natural iron). The

decrease of isomer shift of the octahedral Fe^{3+} in the amorphous state can be explained by the decrease from the crystalline Fe_a^{3+}–O bond distance resulting in an increase of *s*-electron density at the nucleus. The B(tet) = 615 cm^{-1} for amorphous RIG materials is slightly larger than the B(tet) = 600 cm^{-1} reported for crystalline garnets. The increase of δ-values indicates a relative increase of Fe^{3+}–O distances (1.866 Å in crystalline RIG) or a decrease of *s*-electron density at the tetrahedral site due to an increase of positive charge at the octahedral Fe^{3+} site. An increase of the Fe–O distance is also indicated by a relatively smaller ligand-field parameter. Interestingly, the increase of the Fe^{3+}–O distance in tetrahedra of amorphous RIG materials indicates an improved symmetry at the Fe^{3+} site because (i) the increase of isomer shift δ-values indicates an improved symmetry at the Fe^{3+}-site (*29*), (ii) the tetrahedral Fe^{3+} absorptions of $^4A_1$ ^4E_g and $^4T_1$ in the amorphous state do not split, whereas they split in crystalline garnets due to distortion, (iii) the tetrahedral absorptions shift to larger frequencies, and (iv) the splitting of the tetrahedral Fe^{3+} band, not very obvious in their spectrum, may be due to an amorphous nature, but the breadth of the band is reduced compared to crystalline garnets.

To summarize the observations, the amorphous RIG materials do not show separate Mössbauer absorptions corresponding to tetrahedral and octahedral Fe^{3+}. The observed isomer shift (δ = 0.34 mm/sec) for amorphous RIG materials is less than octahedral (δ = 0.47 mm/s) and greater than tetrahedral Fe^{3+} (δ = 0.24 mm/s) in crystalline garnets. An increase of *s*-electron density at the ^{57}Fe nucleus resulting from a decrease in the Fe–O distance in the amorphous state is clearly evident from the decrease of the δ-value for the octahedron. The decrease of the Fe–O distance is also supported by an increase of Δ in the amorphous state. Therefore, this leads to the conclusion of a contraction of the octahedron in the amorphous state. Similarly, the increase of isomer shift values and B(tet) values along with smaller ligand-field parameters leads to the conclusion of expansion of tetrahedra. Any systematic variation of δ(oct), δ(tet), B(oct), and B(tet) values within the amorphous state (samples heat-treated in the range 450 to 600°C) is not detected. The amorphous state can be visualized by the modification and rearrangements of the crystalline garnet lattice. In the crystalline state, the complex garnet structure with a high percentage of shared edges results in relatively high density. The polyhedral edges shared in the garnet structure (Fig. 1) are: tetrahedra share two edges with triangular dodecahedra, octahedra share six edges with dodecahedra. The triangular dodecahedron has shared edges, two with tetrahedra, four with octahedra, and four with other dodecahedra. In the amorphous state, an overall increase of specific volume is associated with relative expansion of tetrahedra and dodecahedra leading to an increase of Fe_d^{3+}–O and R_c^{3+}–O bond distances whereas the relative contraction of octahedra leads to the decrease of the Fe_a^{3+}–O bond distance. These results are also corroborated by the ferrimagnetic resonance studies and the interesting magnetic behavior of these garnets with low dimensions (*30*).

4. Conclusions

The ultrafine rare earth iron garnets of 1.0- to 1.5-nm crystallite size exhibit IR absorptions comparable to crystalline lighter rare earth iron garnets with expanded lattices, suggesting an increase of specific volume in low dimensions. The specific volume change is attributed to the modifications of various oxygen polyhedra in the ultrafine amorphous state. The proposed energy level scheme of $3d^5$ for Fe^{3+} in tetrahedral and octahedral coordination in these ultrafine

amorphous materials is a modification of the energy level scheme for ultrafine crystalline materials. The greater Racah parameters and Mössbauer isomer shift values for tetrahedral Fe^{3+} indicate an increase of the Fe_d–O bond distance in FeO_4 tetrahedra. The smaller ligand-field parameters Δ(tet) support the observation. The lower value of B(oct) and the larger Δ(oct) suggest the decrease of the Fe_a–O distance in FeO_6 octahedra. The ultrafine rare earth iron garnets of 10- to 35-nm crystallite size exhibit absorption frequencies and spectral parameters comparable to single crystal and bulk polycrystalline garnets.

References

1. W. V. Nicholson and G. Burns, *Phys. Rev.* **133,** 1568 (1964).
2. L. S. Lyubutin and L. G. Lyubutina, *Sov. Phys. Crystallogr.* **15,** 708 (1971).
3. P. Köhler and G. Amthauer, *J. Solid State Chem.* **28,** 329 (1979).
4. G. Amthauer, V. Gönzler, S. S. Hafner, and D. Reinen, *Z. Kristallogr.* **161,** 167 (1982).
5. G. Menzer, *Z. Kristallogr.* **69,** 300 (1929).
6. S. C. Abrahams and S. Geller, *Acta Crystallogr.* **11,** 437 (1958).
7. G. A. Novak and G. V. Gibbs, *Amer. Mineral.* **56,** 791 (1971).
8. F. Euler and J. Bruce, *Acta Crystallogr.* **19,** 971 (1965).
9. D. L. Wood and J. P. Remeika, *J. Appl. Phys.* **38,** 1038 (1967).
10. G. H. Dieke, "Spectra and Energy Levels of Rare Earth Ions in Crystals," Interscience, New York (1968).
11. A. M. Clogston, *J. Appl. Phys.* **31,** 198S (1960).
12. K. A. Wickersheim and R. A. Lefever, *J. Chem. Phys.* **36,** 844 (1962).
13. G. B. Scott and J. L. Page, *Phys. Status Solidi* (b) **79,** 203 (1977).
14. N. T. McDevitt, *J. Opt. Soc. Am.* **59,** 1240 (1969).
15. K. A. Wickersheim, R. A. Lefever, and B. M. Hanking, *J. Chem. Phys.* **32,** 271 (1960).
16. J. J. Van Loef, *Physica* **22,** 2102 (1966).
17. G. A. Sawatzky, F. Van der Woude, and A. H. Morrish, *Phys. Rev.* **183,** 383 (1969).
18. A. H. Morrish and K. Haneda, *J. Magn. Magn. Mater.* **35,** 105 (1983).
19. K. Haneda, *Can. J. Phys.* **65,** 1233 (1987).
20. V. K. Sankaranarayanan and N. S. Gajbhiye, *Thermochim. Acta* **153,** 337 (1989).
21. V. K. Sankaranarayanan and N. S. Gajbhiye, *J. Amer. Ceram. Soc.* **73,** 1301 (1990).
22. M. Rappaz, C. Sollraird, A. Chatelain, and L. A. Boatner, *Phys. Rev. B* **21,** 906 (1980).
23. H. J. Wasserman and J. S. Vermaak, *Surf. Sci.* **32,** 168 (1972).
24. B. Cockayne, *J. Amer. Ceram. Soc.* **49,** 204 (1966).
25. Y. Tanabe and S. Sugano, *J. Phys. Soc. (Japan)* **9,** 753 (1954).
26. P. G. Manning, *Canad. Mineral.* **10,** 657 (1970); **12,** 826 (1972).
27. R. K. Moore and W. B. White, *Canad. Mineral.* **12,** 791 (1972).
28. C. K. Jorgensen, "Orbitals in Atoms and Molecules," Academic Press, London (1962).
29. A. K. Bandhyopadhyay, J. Zarcycky, P. Auric, and J. Chappert, *J. Noncryst. Solids* **40,** 353 (1980).
30. V. K. Sankaranarayanan and N. S. Gajbhiye, *J. Magn. Magn. Mater.* **92,** 217 (1990).